Hindawi
Mathematical Problems in Engineering
Volume 2017, Article ID 1428137, 11 pages
https://doi.org/10.1155/2017/1428137

Research Article

Similarity Solutions of the MHD Boundary Layer Flow Past a Constant Wedge within Porous Media

Ramesh B. Kudenatti,[1] Shreenivas R. Kirsur,[2] Achala L. Nargund,[3] and N. M. Bujurke[4]

[1]*Department of Mathematics, Bangalore University, Bangalore 560 001, India*
[2]*Department of Mathematics, Gogte Institute of Technology, Belagavi 590 008, India*
[3]*P. G. Department of Mathematics and Research Centre in Applied Mathematics, MES College, Malleswaram, Bangalore 560 003, India*
[4]*Department of Mathematics, Karnatak University, Dharwad 580 003, India*

Correspondence should be addressed to Ramesh B. Kudenatti; ramesh@bub.ernet.in

Received 25 September 2016; Revised 25 November 2016; Accepted 13 December 2016; Published 19 January 2017

Academic Editor: Hang Xu

The two-dimensional magnetohydrodynamic flow of a viscous fluid over a constant wedge immersed in a porous medium is studied. The flow is induced by suction/injection and also by the mainstream flow that is assumed to vary in a power-law manner with coordinate distance along the boundary. The governing nonlinear boundary layer equations have been transformed into a third-order nonlinear Falkner-Skan equation through similarity transformations. This equation has been solved analytically for a wide range of parameters involved in the study. Various results for the dimensionless velocity profiles and skin frictions are discussed for the pressure gradient parameter, Hartmann number, permeability parameter, and suction/injection. A far-field asymptotic solution is also obtained which has revealed oscillatory velocity profiles when the flow has an adverse pressure gradient. The results show that, for the positive pressure gradient and mass transfer parameters, the thickness of the boundary layer becomes thin and the flow is directed entirely towards the wedge surface whereas for negative values the solutions have very different characters. Also it is found that MHD effects on the boundary layer are exactly the same as the porous medium in which both reduce the boundary layer thickness.

1. Introduction

The research in MHD boundary layer flow has many important engineering applications such as power generators, the cooling of reactors, polymer industry, and spinning of filaments. In industrial applications, when sheets or filaments are made to cool, these get stretched. This cooling can be controlled by applying the magnetic field; we would then expect the final products with desired shapes. Because of these significant applications, Pavlov [1] considered the boundary layer flow of a conducting incompressible viscous fluid due to deformation of an elastic surface in uniformly applied magnetic field. Andersson [2] studied the MHD boundary layer flow of a viscous fluid past a stretching surface and showed that external magnetic field has the same effect on the flow as the viscoelasticity. There are numerous papers available in the literature on classical MHD boundary layer flows (Watanabe and Pop [3]; Chaturvedi [4]) and along with heat and mass transfer flows (Yih [5], Sobha and Ramkrishna [6], Aly et al. [7], etc.). Joneidi et al. [8] undertook the study of heat and mass transfer of viscous fluid in an electrically conducting fluid and showed that MHD decreases the boundary layer thickness. Hayata et al. [9] have modeled the two-dimensional magnetohydrodynamic boundary layer flow in a channel with porous walls, and they considered Maxwell's fluid in the porous space between the channel walls and solved the governing ordinary differential equations by homotopy analysis method. The effects of all embedded flow parameters on the dimensionless velocity components and temperature along with Nusselt number are analyzed. Pantokratoras [10] has obtained the exact solutions to the boundary layer flow along a vertical plate in the

presence of the applied magnetic field and obtained analytical expressions in terms of series form for Blasius-Sakiadis and Sakiadis flows.

Xu et al. [11] have investigated the boundary layer flow and heat transfer in an incompressible viscous electrically conducting fluid that is caused by impulsive stretching of the surface and used a well-developed homotopy analysis method. They showed that the magnetic parameter reduces the boundary layer thickness but enhances thermal boundary layer thickness.

The study of fluid flows and mass transfer problems has significant applications in a wide variety of geophysical and engineering application such as flow of ground water energy storage and chemical reactors (Nield and Bejan [12]; Ingham et al. [13]). Some materials such as sintered bronze or metal sheet perforated with numerous small holes are porous. If these materials are used as the boundary of a region of fluid flow and free stream velocity is maintained on the other side away from the flow, the fluid will be sucked/injected through the boundary. Then the appropriate boundary conditions for the flow region is the normal component of the relative velocity of fluid and surface at the boundary should be equal to some value determined by the porosity that is represented by the normal relative velocity α ($\alpha > 0$ for suction and $\alpha < 0$ is injection) (Batchelor [14]). Yao [15] studied the Falkner-Skan flow over a wedge in a porous medium using the approximate analytical solution given by homotopy analysis. Guedda et al. [16] have explored numerically for the case of MHD mixed boundary layer flow over a vertical flat plate in a porous medium and shown that there exist multiple solutions for specific parameters.

It is noticed that the exact solutions in boundary layer flow problems through similarity transformations are very few. In fact the classical Falkner-Skan equation,

$$f'''(\eta) + f(\eta) f''(\eta) + \beta\left(1 - f'^2(\eta)\right) = 0, \tag{1}$$

with the boundary conditions

$$\begin{aligned} f(0) &= 0, \\ f'(0) &= 0, \\ f'(\infty) &= 1, \end{aligned} \tag{2}$$

admits no analytical solution, because the nonlinearities in the equation and appearance of the pressure gradient parameter make the above system susceptible to obtain an analytical solution. However, when one or both of the initial conditions are nonzero and for $\beta = -1$, the above system yields an analytical solution in the form of error and exponential functions (Sachdev et al. [17]). Exploring this known analytical solution, they modified and rewrote it to obtain an exact solution of the Falkner-Skan equation for all possible values of β. Pioneered by this work, Kudenatti et al. [18] obtained an analytical solution of the MHD Falkner-Skan equation for various values of β and the Hartmann number M and explored that their solutions are consistent with the numerical solutions. At present, an analytical evidence for two-dimensional boundary layer flow over a wedge with an embedded permeability is not yet reported and that requires a credible mechanism for its analysis. To facilitate this, we follow the similar rational mathematical analysis pioneered by Sachdev et al. [17]. Nevertheless, encouraged by the insights obtained previously from the exact solution of the Falkner-Skan equation, we investigate the nature of the boundary layer flow and also briefly describe subsequent far-field behavior asymptotically. Considering the influence of favorable pressure gradient parameter, Volchkov et al. [19] have shown that the dynamic boundary layers satisfy their asymptotic conditions when skin-friction coefficient has no dependence on Reynolds number as at asymptotic suction of the boundary layer through the porous wall. They also found the analogy between the suction through the porous wall and the boundary layer of the accelerated flow; there is cross-flow directed from the outer boundary to the wall.

More recently, Rashidi and Erfani [20] discussed the similarity solution of MHD Hiemenz flow against a flat with variable wall temperature in porous media. We have extended the work of Rashidi and Erfani [20] for the Falkner-Skan flow by introducing the non-Darcy velocity in the boundary layer equations.

An analysis has been undertaken in order to investigate the effect of permeability on the boundary layer flow of an incompressible electrically conducting fluid over a stationary wedge in the presence of transverse magnetic field. The boundary layer Falkner-Skan flow is associated with four physical parameters which exhibit different solution nature. We aim to revisit some of these solutions and to find velocity profiles and skin friction in each case and determine corresponding flow structure.

The organization of the paper is as follows. In Section 2, we describe the mathematical modeling of the problem under discussion, and derive its governing equation, that is, the Falkner-Skan equation along with appropriate boundary conditions. We also give an exact solution of Falkner-Skan equation for certain parameters. Section 3 devotes to derive an exact solution of the Falkner-Skan equation for all physical parameters. We modified the known exact solution for $\beta = -1$ to give the solution for general values of β and M and the permeability parameter Ω and discuss the dynamics of the velocity profiles. Section 4 contains an asymptotic solution in the limit of large η and obtains the solution of the linearized differential equation in the form of confluent hypergeometric functions, and we discuss the results obtained in this section. The last section summarizes the important results of this work.

2. Model

We consider the MHD two-dimensional viscous and incompressible flow over a constant wedge through porous media. The x-axis is measured along the direction of the wedge surface, and y-axis is measured normal to the flow and fluid is occupying the half-space $y > 0$. For a large Reynolds number, the viscosity effects are confined to the wedge surface, and this clearly divides into near field where the viscosity plays a dominant role and far field where the zero-shear viscosity is important. The constant wedge is entirely immersed inside

a porous matrix which is subject to applied magnetic field $B(x)$ (applied normal to the flow). Let $\vec{q} = (u, v)$ be the velocity vector in which u and v are velocity components in x- and y-directions and this velocity field develops due to the interaction of the electromagnetic field inside the porous medium. Thus, the MHD for two-dimensional flow with usual notations are

$$\nabla \cdot \vec{q} = 0, \tag{3}$$

$$\frac{1}{\epsilon^2}(\vec{q} \cdot \nabla)\vec{q} = -\frac{1}{\rho}\nabla p + \frac{\mu_e}{\rho}\nabla^2\vec{q} - \frac{\mu}{\rho K}\vec{q} + \frac{1}{\rho}\vec{J} \times \vec{B}, \tag{4}$$

where ρ is the fluid density, ϵ is the porosity, p is the pressure, μ_e is the effective viscosity, for simplicity we consider it to be identical to the dynamic viscosity μ, K is the permeability of the porous medium, and $\vec{J} \times \vec{B}$ $(=\sigma(E + \vec{q} \times B) \times B)$ is a body force. This body force represents the coupling between the magnetic field and the fluid motion which is called Lorentz force. The induced magnetic field is assumed to be negligible. This assumption is justified by the fact that the magnetic Reynolds number is very small. This plays a vital role in some engineering problems where the conductivity is not large in the absence of an externally applied field. It has been taken that $E = 0$. Thus the Lorentz force is given by

$$\vec{J} \times \vec{B} = -\sigma B^2 \vec{q}. \tag{5}$$

Since the magnetic drag is a body force on the moving fluid and not on the porous medium, the right-hand side of (5) must be multiplied by the factor ϵ^{-1}. Then from (4) and (5), we obtain

$$\frac{1}{\epsilon^2}(\vec{q} \cdot \nabla)\vec{q} = -\frac{1}{\rho}\nabla p + \frac{\mu_e}{\rho}\nabla^2\vec{q} - \frac{\mu}{\rho K}\vec{q} - \frac{\sigma B^2(x)}{\rho\epsilon}\vec{q}. \tag{6}$$

Let $U(x)$ be the velocity of the mainstream flow along x-direction outside the boundary layer. The key idea involved in making the boundary layer approximation is that the viscosity effects are dominant in the adjacent to the surface. If δ is the thickness of the boundary layer, then $\delta \ll L$, where L is the characteristic horizontal length. This implies on making an order of magnitude estimate of each term with $\delta \ll L$. Hence v is much smaller than u. Also the other basic approximation is $|\partial u/\partial y| \gg |\partial u/\partial x|$. Further, it is also assumed that $|\partial p/\partial y| \ll |\partial p/\partial x|$ in (6) meaning that the pressure p in the boundary layer is a function of x only (to the approximation). With $\delta \ll L$, the term $\partial^2 u/\partial x^2$ can be neglected in comparison with $\partial^2 u/\partial y^2$. With these assumptions we close the derivation and corresponding momentum and continuity equations are given by

$$\frac{\partial u}{\partial x} + \frac{\partial v}{\partial y} = 0, \tag{7}$$

$$\frac{1}{\epsilon^2}\left(u\frac{\partial u}{\partial x} + v\frac{\partial u}{\partial y}\right) = -\frac{1}{\rho}\frac{\partial p}{\partial x} + \nu\frac{\partial^2 u}{\partial y^2} - \frac{\nu}{K}u - \frac{\sigma B^2(x)}{\rho\epsilon}u, \tag{8}$$

$$\frac{\partial p}{\partial y} = 0, \tag{9}$$

To determine the pressure distribution, the velocity at the edge of the boundary layer is equal to the mainstream flow $U(x)$ and by Bernoulli's theorem, the pressure would be constant in the inviscid flow influenced by the porous media and applied magnetic field; that is,

$$\frac{U(x)}{\epsilon^2}\frac{dU(x)}{dx} = -\frac{1}{\rho}\frac{dp}{dx} - \frac{\mu}{\rho K}U(x) - \frac{\sigma B^2}{\rho\epsilon}U(x). \tag{10}$$

Plugging (10) in (8), we get the MHD boundary layer equation as

$$\frac{1}{\epsilon^2}\left(u\frac{\partial u}{\partial x} + v\frac{\partial u}{\partial y}\right) = \frac{1}{\epsilon^2}U(x)\frac{dU(x)}{dx} + \nu\frac{\partial^2 u}{\partial y^2} - \frac{\nu}{K}(u - U(x)) - \frac{\sigma B^2(x)}{\rho\epsilon}(u - U(x)). \tag{11}$$

All terms on the right-hand side (from left to right) represent the effects of the mainstream forcing, the viscous forces, the porous medium, and the magnetic interaction on the boundary layer flow. The mainstream velocity $U(x)$ is expected to obey the power-law relation $U(x) = U_\infty x^m$, where U_∞ is constant and m defines the strength of pressure gradient. The variations of the m will be discussed later. The relevant boundary conditions for the above model are

$$\begin{aligned} &\text{at } y = 0: \quad u = 0, \\ &\qquad\qquad\quad v = V_w, \\ &\text{as } y \longrightarrow \infty: \quad u \longrightarrow U(x). \end{aligned} \tag{12}$$

In (12), the condition on u on the surface signifies that the wedge surface is at rest, and V_w is the mass transpiration parameter. The conditions on the velocity at infinity mean that the velocity approaches the mainstream flow far-away from the wedge surface. Thus, the main boundary layer effects are restricted to the immediate neighborhood of the surface. System (11) and (12) allows reducing both dependent and independent variables to one each by the following similarity transformations. This is further evidenced by the similar

velocity profiles existing in the boundary layer for any x in the streamwise direction. Accordingly, we define

$$\psi = \sqrt{\frac{2\nu x U(x)\,\epsilon^2}{1+m}}\, f(\eta),$$
$$\eta = \sqrt{\frac{(1+m)\,U(x)}{2\epsilon^2 \nu x}}\, y, \tag{13}$$

where the stream-function $\psi(x, y)$ is defined as

$$(u, v) = \left(\frac{\partial \psi}{\partial y}, -\frac{\partial \psi}{\partial x}\right); \tag{14}$$

from system (11) to (12), we get

$$f'''(\eta) + f(\eta) f''(\eta) + \beta\left(1 - f'^2(\eta)\right) - \left(\Omega + M^2\right)\left(f'(\eta) - 1\right) = 0, \quad \prime = \frac{d}{d\eta} \tag{15}$$

with the boundary conditions

$$f(0) = \alpha, \quad f'(0) = 0, \quad f'(+\infty) = 1. \tag{16}$$

Here (15) is the modified Falkner-Skan equation that accounts MHD and porous of the surface. Here $f(\eta)$ is the nondimensional stream-function, and η is a new similarity variable, α $(=-(1/\epsilon)\sqrt{2x/(m+1)\nu U(x)}V_w)$ is the suction/injection parameter, $\alpha > 0$ represents suction, and $\alpha < 0$ is the injection, whereas $\alpha = 0$ is impermeable of the wedge surface. Also β $(=2m/(1+m))$ is nonlinear pressure gradient parameter, $\beta > 0$ is the favorable, and $\beta < 0$ is the adverse pressure gradient, whereas $\beta = 0$ is the two-dimensional Blasius flow over a flat plate. Parameter M $(=B_0^2\sqrt{2\sigma\epsilon/\rho U_\infty(m+1)})$ is the magnetic (Hartmann number) parameter which is the ratio of electromagnetic force to the viscous force and Ω $(=2\epsilon^2(U_\infty/\nu)^{(m-2)}/K(m+1)\mathrm{Re}_x^{(m-1)})$ is permeability, and Re_x $(=U_\infty x/\nu)$ is the local Reynolds number. For $\beta = 0 = M = \Omega$, the above problem reduces to the Blasius flow that describes a two-dimensional flow over a flat plate with mass transfer and is studied by several investigators with different cases and hence no comment is needed. For $M = \alpha = \Omega = 0$, the above system reduces to the classical Falkner-Skan system.

Twice integration of (15) with $\beta = -1$ and $\Omega = 0 = M$ gives the Riccati type equation:

$$2f'(\eta) + f^2(\eta) = \eta^2 + 2\Delta\eta + \alpha^2, \tag{17}$$

where $\Delta = f''(0)$. The solution of (17) is given by

$$f(\eta) = \eta + \Delta + \frac{(\alpha - \Delta)\, e^{-(\eta^2/2 + \Delta\eta)}}{1 + (\alpha - \Delta)(1/2)\, e^{\Delta^2/2}\sqrt{\pi/2}\left(\mathrm{erf}\left((\eta + \Delta)/\sqrt{2}\right) - \mathrm{erf}\left(\Delta/\sqrt{2}\right)\right)}, \tag{18}$$

provided

$$f''(0) = \Delta = \pm\sqrt{-2 + \alpha^2}. \tag{19}$$

We note from (19) that the Falkner-Skan equation (15) admits the dual solutions for $\alpha > \sqrt{2}$ and no solution when $\alpha < \sqrt{2}$. For $\alpha = \sqrt{2}$ there exist a trivial solution for the Falkner-Skan equation and is given by $f(\eta) = \eta$ which demarcates the boundary layer structure. In any case, solutions of the Falkner-Skan equation have a boundary layer character; in fact these are the solutions of the Navier-Stokes equations in simplified form. The above solution can be taken by Kudenatti and Awati [21], but for the completeness of the paper it is given again. We now device the method for obtaining an exact solution of the equation by modifying the above known solution for values of β, Ω, and M and recover the known closed form solution as a special case.

3. Exact Solution

The exact solution (18) can be modified and rewritten as

$$f(\eta) = \eta + \Delta + \frac{(\alpha - \Delta)}{G(\eta)}, \tag{20}$$

where $G(\eta)$ is the new stream-function. The above form exhibits a very interesting solution nature that has not been reported so far. The above form makes it possible to give an exact solution of the problem for all values of β, M, and Ω including the case $\beta = -1$. Substituting the modified form (20) into the Falkner-Skan system (15) and (16), we get

$$G^2 G''' + G'^2\left((-2 + \beta)(\alpha - \Delta) + 6G'\right) - G\left(2(\Delta + \eta)G'^2\right) + (-\alpha + \Delta)G'' + 6G'G'' + G^2\left(-\left(M^2 + 2\beta + \Omega\right)G' + (\Delta + \eta)G''\right) = 0, \tag{21}$$

with the boundary conditions

$$G(0) = 1, \quad G'(0) = \frac{1}{\alpha - \Delta}, \quad G'(+\infty) = 0, \tag{22}$$

where $G = G(\eta)$. For $\beta = -1$ and $\Omega = 0 = M$, solution of (21) is given by

$$G(\eta) = e^{(\eta^2/2+\Delta\eta)}\left(1 + (\alpha-\Delta)\,e^{\Delta^2/2}\sqrt{\frac{\pi}{8}}\left(\operatorname{erf}\left(\frac{\eta+\Delta}{\sqrt{2}}\right) - \operatorname{erf}\left(\frac{\Delta}{\sqrt{2}}\right)\right)\right). \tag{23}$$

The error and exponential functions in (23) are entire functions that can be expanded using Taylor series about $\eta = 0$ and have an infinite radius of convergence. Thus, the series representation of the solution (23) becomes the main clue for further similar analysis for general values of β, M, and Ω. Expecting the similar series representation, it is natural to express the stream-function $G(\eta)$ as

$$G(\eta) = \sum_{n=0}^{\infty} a_n \eta^n \tag{24}$$

for general β, M, and Ω. For obtaining the coefficients a_n, substituting (24) with $a_0 = 1$ and $a_1 = 1/(\alpha - \Delta)$ in hand into (21) and equating the coefficients of various powers of η to zero, we get

$$\begin{aligned} a_3 &= \left(\frac{1}{6(\alpha-\Delta)^3}\right)\left(-6 + \Delta^2\left(M^2+\beta+\Omega\right)\left(1+M^2+\beta+\Omega\right)\left(\alpha^2-2\alpha\Delta\right) + \alpha^2 - 2(\alpha-\Delta)^2\left(-6+\alpha^2-\alpha\Delta\right)a_2\right), \\ a_4 &= \frac{1}{12}\left((\Delta-\alpha\lambda)\,a_1^3 + a_1^2\left(1+M^2+2\beta+\Omega-12a_2\right) + a_2\left(-1+M^2+2\beta+\Omega+12a_2\right) - 3\alpha a_3 \right. \\ &\quad \left. + a_1\left(\left((-1+2\beta)\Delta + \alpha\left(3+\lambda-2\beta(1+\lambda)\right)\right)a_2 + 12a_3\right)\right), \end{aligned} \tag{25}$$

and in general, the recurrence relation is

$$\begin{aligned} a_{n+3} = \frac{-1}{(n+1)(n+2)(n+3)}\Bigg(&\sum_{j=0}^{n-1}\sum_{k=0}^{n-j}(j+1)(j+2)(j+3)\,a_k a_{n-j-k} a_{j+3} \\ &+ \sum_{j=0}^{n}\Bigg(-(\Delta-\alpha)(j+1)\left((j+2)\,a_{n-j}a_{j+2} - (2-\beta)(n-j+1)\,a_{j+1}a_{n-j+1}\right) \\ &- \sum_{j=0}^{n}\sum_{k=0}^{j}(k+1)(j-k+1)\left(2\Delta a_{n-j} - 6(n-j+1)\,a_{n-j+1}\right)a_{k+1}a_{j-k+1} \\ &+ \sum_{j=0}^{n}\sum_{k=0}^{n-j}\Big((j+1)\left(a_{j+1}\left(j-2\beta-J^2+\Omega\right) + \Delta(j+2)\,a_{j+2}\right)a_k a_{n-j-k} \\ &- (k+1)\left(6(j+1)(j+2)\,a_{j+2} + 2(n-j-k)\,a_j\right)a_{k+1}a_{n-j-k}\Big)\Bigg)\Bigg) \end{aligned} \tag{26}$$

for $n = 1, 2, 3, \ldots$. It is observed that all the coefficients a_n have been obtained in terms of unknown parameter a_2 and all physical parameters β, α, M, and Ω. And also note that the definition of Δ $(=\sqrt{\alpha^2-2})$ that was obtained in (19) for $\beta = -1$ and $M = 0 = \Omega$ remains the same even for other values of these parameters. The free parameter a_2 remains unknown because of an end condition in (22); this unknown a_2 must be found in such a way that the derivative condition at far distance is satisfied (i.e., $f'(\infty) = 1$). Following (20) and (24), the unknown a_2 is related to $f''(0)$ through

$$a_2 = \frac{-1}{2(\alpha-\Delta)}\left(f''(0) - \frac{2}{(\alpha-\Delta)}\right), \tag{27}$$

where $f''(0)$ is also unknown. To determine a_2 or $f''(0)$, integrating the MHD Falkner-Skan equation (15) across the boundary thickness using the boundary conditions (16), we get

$$\begin{aligned} &\int_0^{\infty}\left(f'(\eta) - f'^2(\eta)\right)d\eta + \beta\int_0^{\infty}\left(1-f'^2(\eta)\right)d\eta \\ &\quad - M_1\int_0^{\infty}\left(f'(\eta)-1\right)d\eta = f''(0) - \alpha, \end{aligned} \tag{28}$$

where $M_1 = (M^2+\Omega)$. Looking at (27) and (28), it is sufficient to determine either a_2 or $f''(0)$. Since $f''(0)$ appears on both sides of (28), it should be found iteratively using suitable initial approximation for it. The initial approximation is taken from the known exact solution (18) for other values of β, M, and Ω. Convergent $f''(0)$ is obtained when the derivative condition at far distance is satisfied, that is, $f'(\eta) \to 1$ as $\eta \to \infty$ (Kudenatti et al. [18]). The values for $f''(0)$ which defines

Table 1: Comparison of the wall-shear stress value $f''(0)$ obtained by solution (29) with numerical solution of the problem.

		$M = 1$					
α	β	$\Omega = 0.1$		$\Omega = 0.5$		$\Omega = 1.0$	
		Exact solution	Numerical solution	Exact solution	Numerical solution	Exact solution	Numerical solution
−2.5	0.5	0.55406	0.55406	0.66494	0.66503	0.79464	0.79464
	1.5	0.86272	0.86327	0.96160	0.95955	1.07365	1.07367
	2.5	1.13996	1.13996	1.22414	1.22549	1.32740	1.32796
−1.5	0.5	0.77682	0.77560	0.92210	0.92251	1.05306	1.05305
	1.5	1.14703	1.14704	1.25278	1.25256	1.38488	1.37664
	2.5	1.46059	1.46067	1.55160	1.55163	1.66086	1.66012
1.5	0.5	2.38869	2.38763	2.50242	2.50222	2.63615	2.63635
	1.5	2.76013	2.76233	2.85672	2.85724	2.97045	2.97048
	2.5	3.07548	3.07696	3.14291	3.15978	3.26147	3.25967
2.5	0.5	3.18651	3.18776	3.28564	3.28547	3.50062	3.50181
	1.5	3.51843	3.51893	3.60425	3.60325	3.70529	3.70484
	2.5	3.80649	3.80645	3.87612	3.88176	3.97309	3.97313

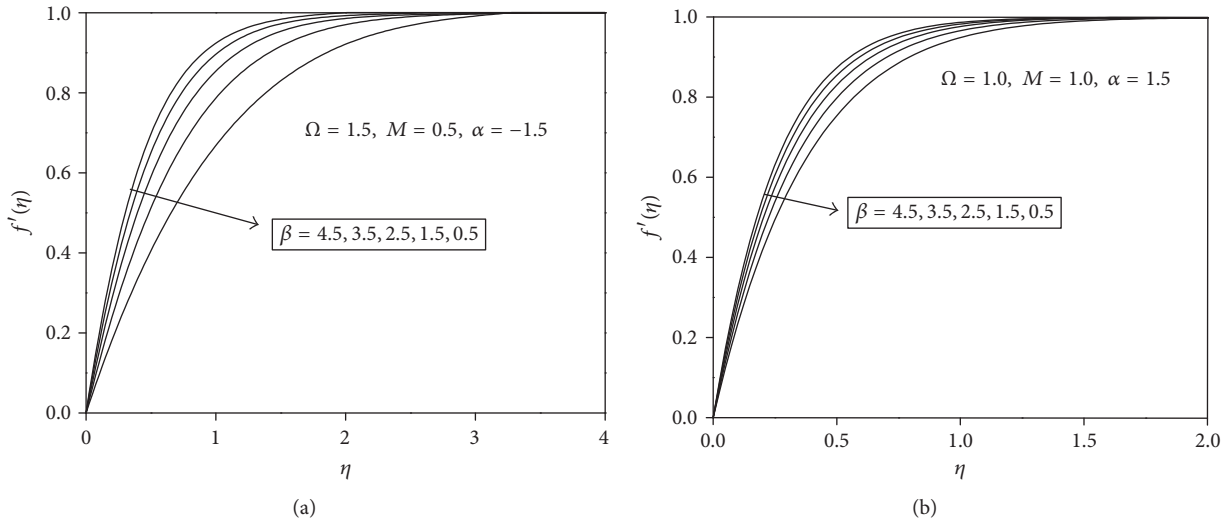

Figure 1: Variation of velocity profiles $f'(\eta)$ with η for different values of $\beta > 0$ for fixed Ω, M, and α.

the skin-friction coefficient thus obtained are consistent with direct numerical solution of the problem. Therefore, we have obtained an exact solution of the Falkner-Skan equation for all the values of β, M, and Ω in the form

$$f(\eta) = \eta + \Delta + \frac{(\alpha - \Delta)}{G(\eta)}, \tag{29}$$

where the convergent power series $G(\eta)$ is given by (24). To assess the efficiency of the present method, we compare the values of $f''(0)$ with that of direct numerical solution of the problem which are given in Table 1, and graphs representing the velocity profiles are given in Figures 1–3. It is observed from table that results from the above method compare well with the numerical solutions for all the values of parameters used in the analysis. Furthermore, for the increasing values for the case of injection ($\alpha < 0$) and suction ($\alpha > 0$), the skin-friction coefficient increases. Also as the permeability parameter Ω increases, it again increases. Therefore, the permeability Ω has a pronounced effect for a given α and pressure gradient β in the presence of magnetic field. Thus with convergent $f''(0)$ in hand, we use solution (29) to plot velocity profiles (first derivative of $f(\eta)$). Again, Figure 1(a) shows the variation of velocity profiles with η for different values of β when other parameters are held constant. These velocity curves are obtained from the exact solution (29). It is observed that for increasing pressure gradient β the thickness of the momentum boundary layer decreases. This is also evident from Figure 1(b) wherein we plot the same graph for slightly bigger values of other constant parameters and found that the velocity curves show the typical behavior, making the boundary layer thickness still thinner. Furthermore, it is evident and well established that the effect of magnetic (Hartman) number is to decrease the boundary layer thickness which is not discussed in detail here. As discussed previously, in Figure 2(a) we investigate the influence of injection parameter ($\alpha < 0$) when other

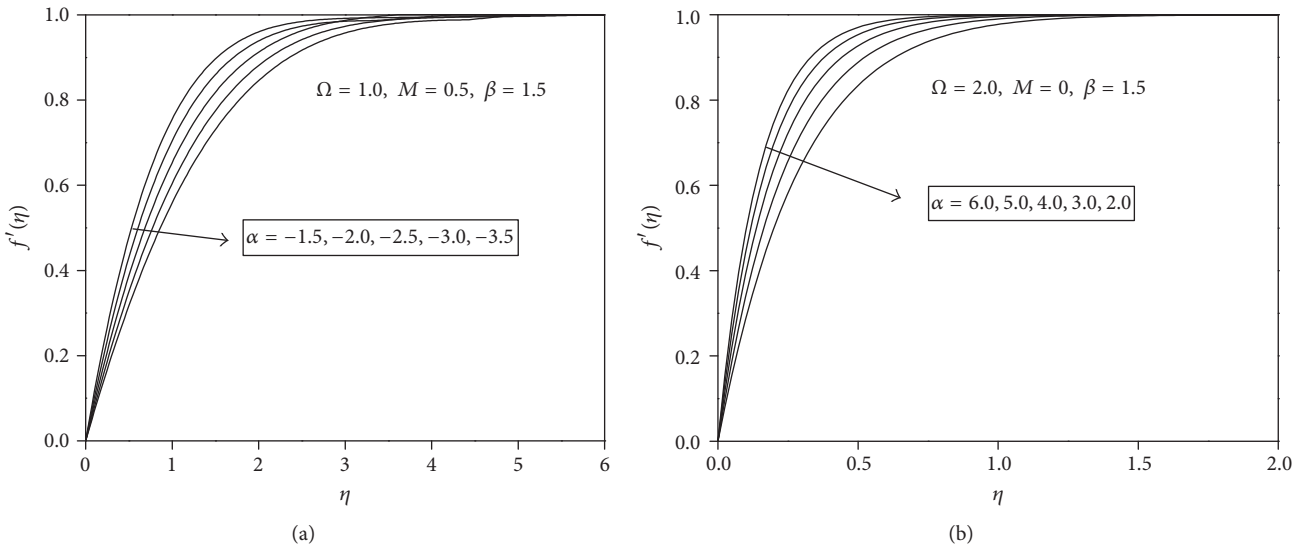

Figure 2: Variation of velocity profiles $f'(\eta)$ with η for different values of α for fixed Ω, M, and β.

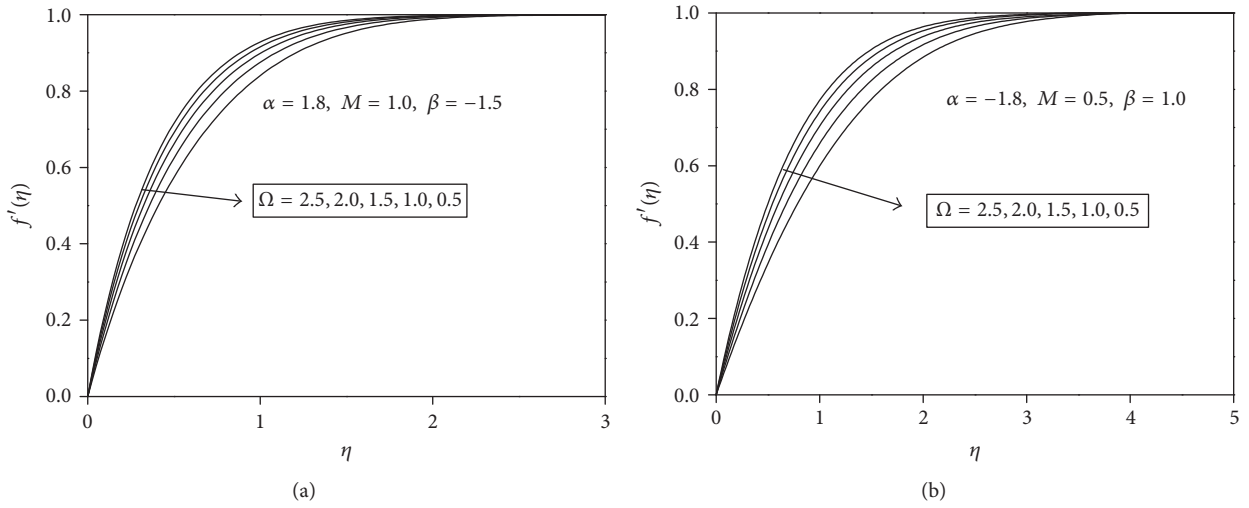

Figure 3: Variation of velocity profiles $f'(\eta)$ with η for different values of permeability parameter Ω for a fixed α, M, and β.

parameters are held constant and found that the mass transfer effectively decreases the boundary layer thickness. Again from Figure 2(b) it is observed that suction parameter ($\alpha > 0$) further reduces boundary layer thickness which is more prominent wherein the effect of permeability is also taken into account ($\Omega = 2$). These typical results have been reciprocated in Figure 3(a) for injection and in Figure 3(b) for suction for different values of permeability parameter Ω. Thus the effect of permeability is to decrease boundary layer thickness. As strength of the permeability increases, the boundary layer thickness again reduces. As it increases, the velocity profiles get closer to the thin boundary layer region, all velocity curves are confined within the thin region. Thus, the suction and permeability of the medium together have a pronounced influence on the velocity profiles.

We have also calculated the two-dimensional boundary layer displacement thickness from our exact solution (29) as

$$\delta_1 = \sqrt{\frac{(m+1)\,U(x)}{2\nu\epsilon^2 x}}\,\delta^* = \int_0^\infty \left(1 - f'(\eta)\right) d\eta. \tag{30}$$

Figures 4(a) and 4(b) display the two-dimensional displacement thickness δ_1 over a range of values of Ω for different values of magnetic number M for fixed α and β. It is observed that displacement thickness increases unboundedly for increasing permeability as well as applied magnetic field.

4. Far-Field Behavior

We investigate the existence of solutions for all flow parameters by examining the asymptotics as $\eta \to \infty$. The derivative

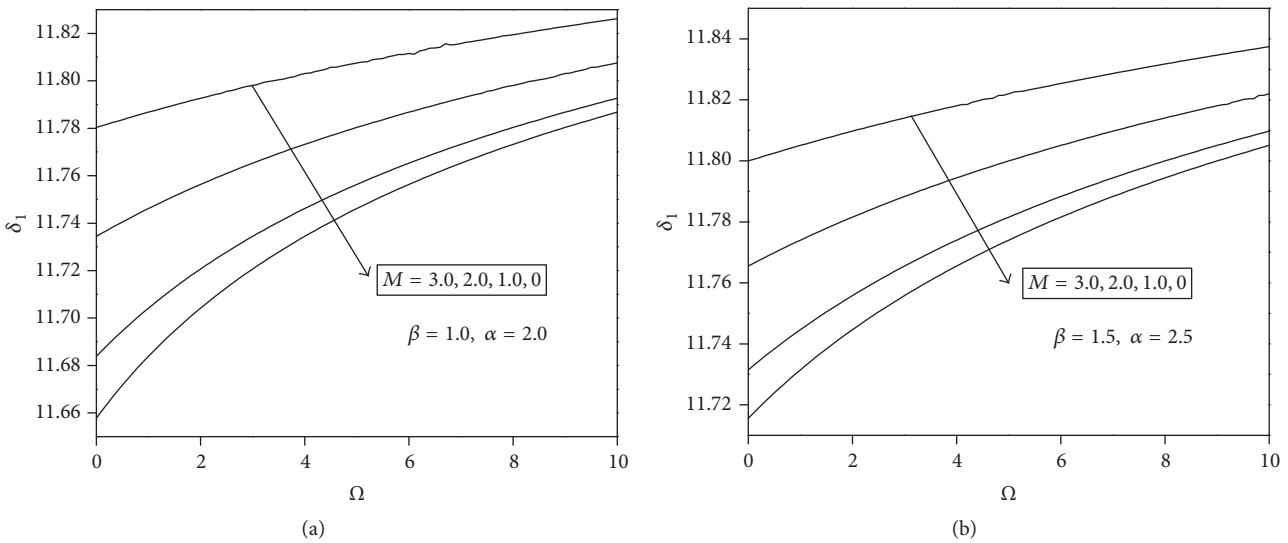

FIGURE 4: Variation of displacement thickness δ_1 with Ω for different values of M for a fixed α and β.

boundary condition at edge of the boundary layer suggests analyzing the local behavior of the solutions; that is, $|f'(\eta) - 1| \ll 1$ as $\eta \to \infty$. This implies to define

$$f(\eta) \sim \alpha + \eta + E(\eta), \tag{31}$$

where $E(\eta)$ and all its derivatives are assumed to be small. Substituting (31) with $f'(\eta) = 1 + E'(\eta)$, $f''(\eta) = E''(\eta)$, and $f'''(\eta) = E'''(\eta)$ into system (15) and (16) and linearizing the resulting ordinary differential equation, we get

$$E'''(\eta) + (\alpha + \eta) E''(\eta) - \left(2\beta + M^2 + \Omega\right) E'(\eta) = 0, \tag{32}$$

and boundary conditions take the form

$$\begin{aligned} E(0) &= 0, \\ E'(0) &= -1, \\ E'(+\infty) &= 0. \end{aligned} \tag{33}$$

Solution of (32) subjected to the conditions (33) is given by

$$E'(\eta) = C_{22}\, {}_1F_1\left(\frac{-B^T}{2}, \frac{1}{2}, -\frac{(\eta+\alpha)^2}{2}\right) - C_{11}\, {}_1U_1\left(\frac{-B^T}{2}, \frac{1}{2}, -\frac{(\eta+\alpha)^2}{2}\right), \tag{34}$$

where

$$\begin{aligned} C_{11} &= \frac{1}{{}_1U_1\left(-B^T/2, 1/2, -\alpha^2/2\right) - C\, {}_1F_1\left(-B^T/2, 1/2, -\alpha^2/2\right)}, \\ C &= \frac{\Gamma\left(1 - B^T/2\right)}{\Gamma(1/2)}, \\ B^T &= 2\beta + \Omega + M^2, \\ C_{22} &= CC_{11}, \end{aligned} \tag{35}$$

where Γ is the Gamma function, $({}_1F_1, {}_1U_1)(\cdot, \cdot, \eta)$ are confluent hypergeometric functions, and C_{11} and C_{22} are known constants obtained from the boundary conditions (33). The asymptotic dependence of $({}_1F_1, {}_1U_1)(\cdot, \cdot, \eta)$ on the parameters as $\eta \to \infty$ will be discussed later. The values for skin friction $f''(0)$ that are obtained by system (31) and (34) are compared with the numerical solution of the Falkner-Skan equation for various values of the physical parameters and are given in Table 2. It is observed that results agree well qualitatively with the numerical solution. Again as discussed previously, for increasing values of α the skin friction obtained by the asymptotic solution also increases, and so is for permeability parameter Ω. Thus, Table 2 resembles closely with Table 1 though both the solutions are obtained using different methods. We plot some of the solutions obtained by the asymptotic solution in Figure 5 for several values of the porous parameter Ω for an adverse pressure gradient β (<0). These results reveal very interesting solution structures which are greatly distinct from $\beta > 0$ velocity profiles (Figure 1). All velocity curves for permeability parameter Ω oscillate finite number of times and eventually satisfy the end condition. Because these solutions exhibit oscillatory behavior, these have both overshoot ($f'(\eta) > 1$) and undershoot ($f'(\eta) < 0$) for some η. The asymptotic solution of the Falkner-Skan equation in the limit of large η clearly indicates that there is a reverse flow in the boundary layer for most of the cases. Thus, for all values of porous parameter, the boundary layer flow can be divided into reverse flow and forward flow, and for a specific Ω, it experiences both of these flows in the boundary layer, but finally for large distance away from the surface, it is only forward flow and satisfies the outer boundary condition. This trend is observed for all values of Ω and is true for other

Table 2: Comparison of the wall-shear stress value $f''(0)$ obtained by the asymptotic solution (31) with numerical solution of the problem.

		$M = 2$					
α	β	$\Omega = 0.3$		$\Omega = 1.5$		$\Omega = 100$	
		Asymptotic solution	Numerical solution	Asymptotic solution	Numerical solution	Asymptotic solution	Numerical solution
	1.0	1.94067	1.74393	2.01452	1.82370	9.59541	9.54691
−1.5	2.5	2.45269	2.10429	2.51481	2.17436	9.73942	9.64240
	3.0	2.60582	2.21529	2.66513	2.28281	9.78698	9.67404
	1.0	2.14065	1.94035	2.21564	2.02153	9.83087	9.78232
−1.0	2.5	2.65963	2.31217	2.72247	2.38303	9.97508	9.87833
	3.0	2.81449	2.42609	2.87443	2.49421	10.0227	9.91015
	1.0	3.17575	2.98078	3.24889	3.05951	10.8331	10.78467
1.0	2.5	3.68438	3.36234	3.74628	3.43084	10.9767	10.88218
	3.0	3.83702	3.47842	3.89618	3.54436	11.0258	10.91448

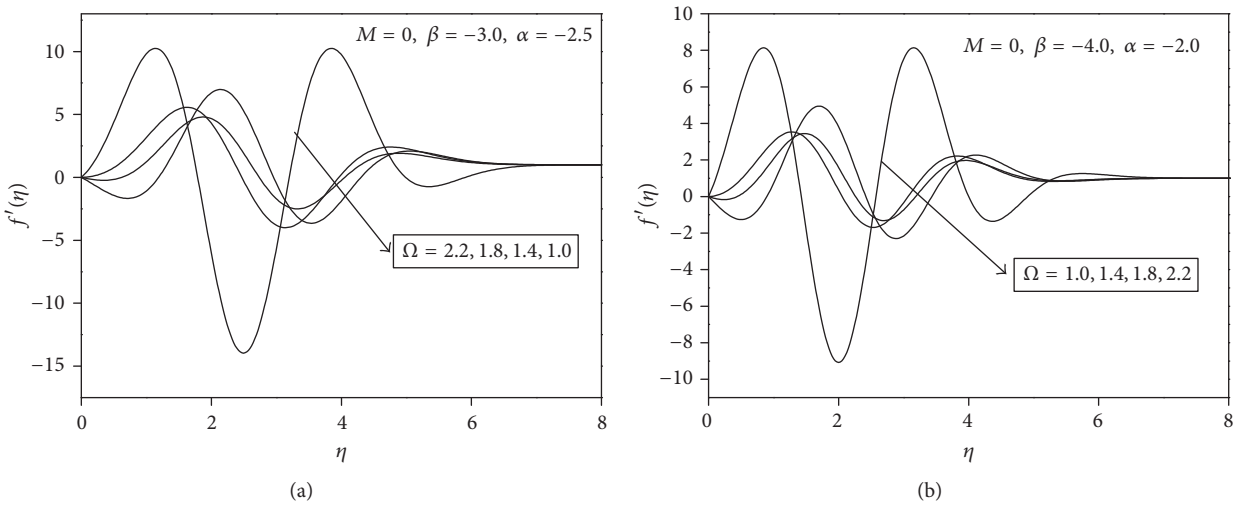

Figure 5: Variation of velocity profiles $f'(\eta)$ that are obtained by asymptotic solution with η for several values of permeability parameter Ω for a fixed α, M, and β.

values of pressure gradient β; see Figures 5(a) and 5(b). These branches of solutions do exist only for the negative values of pressure gradient parameters.

5. Discussion and Conclusion

The similarity solutions of the MHD Falkner-Skan equation are obtained for all physical parameters in terms of a convergent series form. This equation describes the MHD flow of a viscous fluid over a wedge immersed in a porous medium in which the wedge has mass transpiration. The solutions mainly encompass the difference between both positive and negative β and α. Note also that the effect of porous matrix is to give friction to the flow and the magnetic field releases energy to the system exactly in the same spirit. The flow is governed by the nonlinear differential equation of order three and is solved by different approaches (Sections 2 and 3 and of course numerically). The validity and efficiency of the solution method are tested for various parametric values of β, M, Ω, and α and compared with the direct numerical solution of the MHD Falkner-Skan equation. We also investigated the nature of the distribution of velocity in the boundary layer region at which the effects of permeability, magnetic number, and mass transfer are taken into account. Numerical values for these parameters are taken which have been extensively used in the previous theoretical studies. In particular, we have taken the range of values for which the solutions are predicted and boundary layer flows are realized. Further, the direct numerical solutions of the MHD Falkner-Skan equation are obtained via finite difference based Keller-box method. This is a standard method for solving nonlinear boundary value problem on a closed interval, in which the Falkner-Skan equation is converted into an equivalent system of first order equations. The outer boundary condition is taken at very large value of η, that is, $\eta_{\max} \gg 1$. The standard central difference schemes are used for the first order equations, and resulting nonlinear algebraic equations are linearized and solved. Our Keller-box code adapts a variable discretization step size to ensure the desired accuracy in a double precision which was set to 10^{-10} in all our computations. This is because a precise value of $f''(0)$ would be required to compare solution with an analytical ones. On the other hand, to enlarge the radius

of convergence of the truncated power series $G(\eta)$ in (24), the Padé approximants which comprise the ratio of two unknown power series have been used to sum the series $G(\eta)$. Following Bender and Orszag [22], all the coefficients in the Padé approximants are uniquely determined. All the boundary layer profiles have been plotted using solution (29) through (24). Thus, all the solutions (namely, velocity profiles and skin friction) obtained analytically compare well with numerical solution of the problem for all parameters investigated.

Furthermore, following Abramowitz and Stegun [23] asymptotic behavior of (34) for large η can be approximated at leading order as

$$E'(\eta) \sim C_{22}\left(\frac{e^{\pm i\pi(-B^T/2)}}{\Gamma\left(1+B^T\right)/2} Z^{B^T/2} + e^{-Z} Z^{-(1+B^T)/2}\right) - C_{11} Z^{B^T/2} + O\left(|Z|^{-R}\right), \tag{36}$$

where C_{11} and C_{22} are constants and $Z = (\eta+\alpha)^2/2$. Equation (36) can be rewritten as

$$E'(\eta) \sim \underbrace{A_{11} Z^{B^T/2}}_{I} + \underbrace{B_{11} e^{-Z} Z^{-(1+B^T)/2}}_{II}, \tag{37}$$

where A_{11} and B_{11} are taken appropriately from (36). Depending on the numerical values of flow parameters (β, M, and Ω), the following analytical conclusions can be made:

(1) If $B^T = 0$, I becomes constant, while II decays asymptotically to zero.

(2) If $B^T > 0$, I diverges algebraically and II converges exponentially to zero; therefore both solutions I and II together lead to convergent solutions. So these velocity profiles satisfy both boundaries but are entirely different in the intermediate values of η.

(3) If $B^T < 0$, both I and II converge to zero in fact very slowly, and we found that existence of velocity profiles in the regime of parameters. In this case, the combination of parameters exhibits a very special solution. Thus, velocity profiles experience oscillatory behavior confirming the reverse flow, which are shown in Figures 5(a) and 5(b).

The analytical and asymptotic simulations provide evidence that the boundary layer profiles do exist for all physical parameters. The rigorous mathematical investigation of all possible regimes of the flow parameters would require many more simulations of the boundary layer flow and in fact a proper simulation. The above self-similar results may be used to extend the present analysis by including the unsteady boundary layer flow situation, which is the interest of the future work. It may be anticipate that a new family of unsteady boundary layer profiles is available, and a detailed investigation into these solutions about overshoot and oscillatory behavior should provide a rich subject for further work.

Competing Interests

The authors declare that there is no conflict of interests regarding the publication of this paper.

Acknowledgments

The authors Ramesh B. Kudenatti and N. M. Bujurke are grateful to the University Grants Commission, New Delhi, India, for providing financial support under a major research project (No. 39-32/2010 (SR)) to carry out work.

References

[1] K. B. Pavlov, "Magnetohydrodynamic flow of an incompressible viscous fluid caused by deformation of a surface," *Magnitnaya Gidrodinamika*, vol. 4, pp. 146–147, 1974.

[2] H. I. Andersson, "MHD flow of a viscoelastic fluid past a stretching surface," *Acta Mechanica*, vol. 95, no. 1, pp. 227–230, 1992.

[3] T. Watanabe and I. Pop, "Hall effects on magnetohydrodynamic boundary layer flow over a continuous moving flat plate," *Acta Mechanica*, vol. 108, no. 1–4, pp. 35–47, 1995.

[4] N. Chaturvedi, "On MHD flow past an infinite porous plate with variable suction," *Energy Conversion and Management*, vol. 37, no. 5, pp. 623–627, 1996.

[5] K. A. Yih, "The effect of uniform suction/blowing on heat transfer of magnetohydrodynamic Hiemenz flow through porous media," *Acta Mechanica*, vol. 130, no. 3-4, pp. 147–158, 1998.

[6] V. Sobha and K. Ramakrishna, "Convective heat transfer past a vertical plate embedded in porous medium with an applied magnetic field," *Journal of the Institution of Engineers: Mechanical Engineering Division*, vol. 84, no. 3, pp. 130–134, 2003.

[7] E. H. Aly, M. Benlahsen, and M. Guedda, "Similarity solutions of a MHD boundary-layer flow past a continuous moving surface," *International Journal of Engineering Science*, vol. 45, no. 2–8, pp. 486–503, 2007.

[8] A. A. Joneidi, G. Domairry, and M. Babaelahi, "Analytical treatment of MHD free convective flow and mass transfer over a stretching sheet with chemical reaction," *Journal of the Taiwan Institute of Chemical Engineers*, vol. 41, no. 1, pp. 35–43, 2010.

[9] T. Hayata, R. Sajjada, Z. Abbasc, M. Sajidd, and A. A. Hendie, "Radiation effects on MHD flow of Maxwell fluid in a channel with porous medium," *International Journal of Heat & Mass Transfer*, vol. 54, pp. 854–862, 2011.

[10] A. Pantokratoras, "Some exact solutions of boundary layer flows along a vertical plate with buoyancy forces combined with lorentz forces under uniform suction," *Mathematical Problems in Engineering*, vol. 2008, Article ID 149272, 16 pages, 2008.

[11] H. Xu, S.-J. Liao, and I. Pop, "Series solutions of unsteady three-dimensional MHD flow and heat transfer in the boundary layer over an impulsively stretching plate," *European Journal of Mechanics. B. Fluids*, vol. 26, no. 1, pp. 15–27, 2007.

[12] D. A. Nield and A. Bejan, *Convection in Porous Media*, Springer, 2nd edition, 1999.

[13] D. Ingham, A. Bejan, E. Mamut, and I. Pop, *Emerging Technologies and Techniques in Porous Media*, Kluwer, Dordrecht, The Netherlands, 2004.

[14] G. K. Batchelor, *An Introduction to Fluid Dynamics*, Cambridge University Press, Cambridge, UK, 2005.

[15] B. Yao, "Approximate analytical solution to the Falkner-Skan wedge flow with the permeable wall of uniform suction," *Communications in Nonlinear Science and Numerical Simulation*, vol. 14, no. 8, pp. 3320–3326, 2009.

[16] M. Guedda, E. H. Aly, and A. Ouahsine, "Analytical and ChPDM analysis of MHD mixed convection over a vertical flat

plate embedded in a porous medium filled with water at 4∘C," *Applied Mathematical Modelling*, vol. 35, no. 10, pp. 5182–5197, 2011.

[17] P. L. Sachdev, R. B. Kudenatti, and N. M. Bujurke, "Exact analytic solution of a boundary value problem for the Falkner-Skan equation," *Studies in Applied Mathematics*, vol. 120, no. 1, pp. 1–16, 2008.

[18] R. B. Kudenatti, S. R. Kirsur, L. N. Achala, and N. M. Bujurke, "Exact solution of two-dimensional MHD boundary layer flow over a semi-infinite flat plate," *Communications in Nonlinear Science and Numerical Simulation*, vol. 18, no. 5, pp. 1151–1161, 2013.

[19] E. P. Volchkov, M. S. Makarov, and A. Y. Sakhnov, "Boundary layer with asymptotic favourable pressure gradient," *International Journal of Heat and Mass Transfer*, vol. 53, no. 13-14, pp. 2837–2843, 2010.

[20] M. M. Rashidi and E. Erfani, "A new analytical study of MHD stagnation-point flow in porous media with heat transfer," *Computers & Fluids*, vol. 40, no. 1, pp. 172–178, 2011.

[21] R. B. Kudenatti and V. B. Awati, "Solution of pressure gradient stretching plate with suction," *Applied Mathematics and Computation*, vol. 210, no. 1, pp. 151–157, 2009.

[22] C. M. Bender and S. A. Orszag, *Advanced Mathematical Methods for Scientists and Engineers*, McGraw-Hill Book, New York, NY, USA, 1978.

[23] M. Abramowitz and I. Stegun, *Handbook of Mathematical Functions*, Dover Publications, 1970.